Studies of defects in combustion synthesized europium-doped LiAl$_5$O$_8$ red phosphor

Vijay Singh [a,*], T.K. Gundu Rao [b]

[a] Laboratoire de Photonique Quantique et Moléculaire, UMR CNRS 8537, Institut d'Alembert-Ecole Normale Superieure de Cachan, 61 avenue du President Wilson, 94235 Cachan, France
[b] R.S.I.C., Indian Institute of Technology, Powai, Mumbai 400 076, India

A R T I C L E   I N F O

A B S T R A C T

Europium-doped LiAl$_5$O$_8$ red phosphor was prepared using a self-propagating (combustion) synthesis. The formation of crystalline LiAl$_5$O$_8$ was confirmed by X-ray diffraction. The morphological aspect of the resulting powders was examined by scanning electron microscopy. Electron spin resonance studies have been carried out in order to study the characteristics of the defect centres and the thermoluminescence (TL) peaks observed in this phosphor. Two types of centres (centre I and centre II) have been identified in LiAl$_5$O$_8$:Eu. Centre I is characteristic of a species exhibiting an isotropic g-value 2.0089 with a line width of 70 G and is assigned to a V-centre. Centre II is also characterized by an isotropic g-value 2.0059 with a line width of about 10 G. Centre II is ascribed to a F$^+$-centre. A room temperature photoluminescence study shows a strong emission line at 613 nm corresponding to the $^5D_0 \rightarrow {}^7F_2$ transition of Eu^{3+} ions.

1. Introduction

LiAl$_5$O$_8$ is used as a host for luminescent materials doped with transition metal ions. The LiAl$_5$O$_8$ doped with transition metal ions, such as Cr^{3+}, Fe^{3+}, Co^{3+}, have been synthesized and their luminescence studies have been reported by different groups [1–4]. However, our investigation shows that reports on LiAl$_5$O$_8$ doped with rare-earth ions are very few. Our interest in the present study is europium-doped LiAl$_5$O$_8$.

Trivalent europium is the most stable state of europium and therefore widely doped in several hosts for producing red colour and bright photoluminescence. Due to these reasons, Eu^{3+} ion is the subject of numerous optical spectroscopic and luminescence investigations for the next generation of displays and lighting devices. Being an important emitter in the red region of the visible spectrum, Eu^{3+} ions have been utilized extensively in electroluminescence panels (EL), plasma display panels (PDP) and high efficiency fluorescent lamps [5–8].

In the recent years, rare-earth activated mixed sulphate, alkaline earth sulphate phosphors have been investigated for elucidating the role of defects formed on self/gamma irradiation as well as the role of actinide dopants in the thermally stimulated

luminescence (TSL) process [9–11]. More recently we have also reported the TSL and electron paramagnetic resonance (EPR) studies on the rare-earth-doped aluminate and sulphide phosphors, wherein the nature of defects formed on irradiation in these phosphors and their role in the thermally stimulated relaxation processes leading to TSL have been investigated [12–14].

In this paper, a facile combustion process was chosen to prepare Eu^{3+}-doped LiAl$_5$O$_8$ phosphor since combustion process is very facile, safe, instantaneous and energy saving. Several thermoluminescence (TL) and ESR studies have shown that defect centres are related to the process of TL in phosphors. Luminescence in these materials is initiated by the release of holes/electrons from defect centres. In the present work, we have investigated the defect centres formed in Eu^{3+}-doped LiAl$_5$O$_8$ phosphor by the use of ESR. We have combined ESR, TL and PL data to obtain information about the presence and decay of various defect centres and luminescence centres in this material.

2. Experimental

2.1. Sample preparation

For the combustion synthesis oxidizer, fuel ratio was calculated based on oxidizing (O) and fuel (F) valencies of the reactants,

* Corresponding author at: Department of Physics, Bhoj College, Kotra, Bhopal-462003, India.
E-mail address: vijayjiin2006@yahoo.com (V. Singh).

keeping O/F = 1, as reported earlier [15]. Eu^{3+}-doped $LiAl_5O_8$ was prepared with the formula $Li_{0.99}Eu_{0.01}Al_5O_8$ [with the source materials 0.1819 g of $Li(NO_3)$, 5 g of $Al(NO_3)_3 \cdot 9H_2O$, 2.1341 g of urea (CH_4N_2O) and dopant (0.0046 g of Eu_2O_3)].

All the reagents were of analytical grade purity. Starting materials were crushed and ground in a dish to form paste. The dish (with the paste) was introduced into a muffle furnace which was maintained at 500 °C. Initially, the paste melted and underwent a dehydration process. This was followed by decomposition with the evolution of large amounts of gas. The mixture was then frothed and swelled thus forming a foam which ruptured with a flame and glowed to incandescence. During incandescence, the foam further swelled to the capacity of the container. The entire combustion process was over in less than 5 min. The dish was taken out and the foamy product was crushed into a fine powder. This powder was white in colour and its properties were evaluated.

2.2. Instruments

Powder XRD pattern was obtained using a Philips X' pert X-ray diffractometer with graphite monochromatized $CuK\alpha$ radiation ($\lambda = 0.15418$ nm) and nickel filter with a scanning step of 0.03°, in the 2θ range of 15–80°. Powder morphology was studied using scanning electron microscopy (SEM, Hitachi S-4300, Japan). Photoluminescence measurements were carried out at room temperature on a Hitachi F-4500 fluorescence spectrophotometer. TSL glow curves were recorded with the usual setup consisting of a small metal plate heated directly using a temperature programmer, photomultiplier (931B), dc amplifier and a millivolt recorder. ESR measurements were carried out on a Varian E-112 E-line Century series X-band ESR spectrometer. TCNE ($g = 2.00277$) was used as a standard for g-factor measurements. Step heat treatments were performed to follow the decay and evolution of the defect centres. These were carried out in situ in the ESR cavity using the Varian variable temperature accessory.

3. Results and discussion

3.1. X-ray diffraction

The formation of crystalline phases of the combustion synthesized $LiAl_5O_8$:Eu was confirmed by powder XRD measurements. Fig. 1a shows the XRD pattern of as-prepared $Li_{0.99}Eu_{0.01}Al_5O_8$. The observed pattern matches with the standard data of the compound (JCPDS file no. 71-1736; Fig. 1b). It was noticed that the loading of Eu (1%) does not create any other impurity phases. It should be pointed out that the mono crystalline phase is possible via a self-propagating (combustion) synthesis even at 500 °C furnace temperature. Therefore, further post-processing for crystallization is not needed.

3.2. Scanning electron microscopy

The morphological aspect of the resulting powders was examined by SEM, which showed that particles are angular and of varying sizes. A magnified portion of Fig. 2a (portion a) is shown in Fig. 2b. High resolution Fig. 2b showed the presence of several nanoparticles within the grains. Portion (c) of Fig. 2c is magnified to obtain Fig. 2d. It was observed from Fig. 2d that angular particles contain non-uniform pores. It is believed that the porosity is formed due to large amount of gases escaping during combustion reactions. It is also clear from Fig. 2a–d that some regions contain pores while some do not. This is due to the
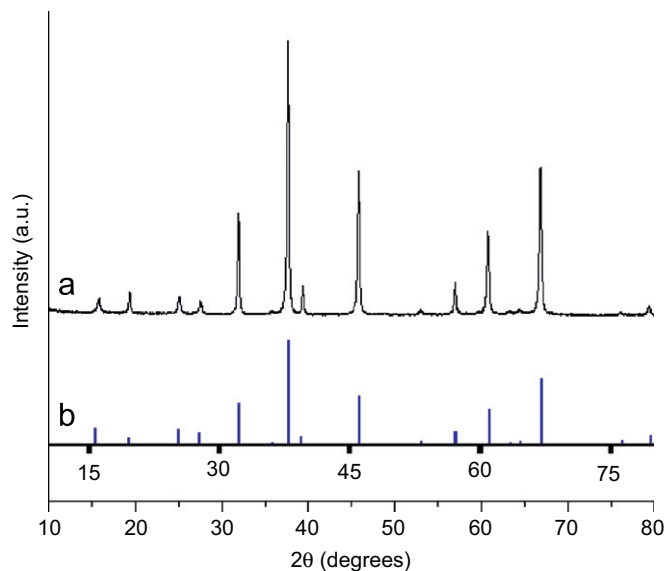

Fig. 1. Powder XRD patterns of (a) $LiAl_5O_8$:Eu and (b) $LiAl_5O_8$ diffraction pattern (JCPDS, no. 71-1736).

non-uniform distribution of temperature and mass flow in the combustion flame. High-resolution SEM micrographs (Fig. 2e and f) showed that the pore diameter ranged from about 300 nm to 1 μm. It should be pointed out that the morphology of Eu-doped $LiAl_5O_8$ (in this work) and undoped $LiAl_5O_8$ [16] are almost the same. This could be due to the very low amount of dopant (Eu 1%) in the host ($LiAl_5O_8$).

3.3. Thermoluminescence and electron paramagnetic resonance studies

An unirradiated freshly prepared $LiAl_5O_8$:Eu sample did not show any glow peak. However, gamma-irradiated (dose = 15 kGy) samples exhibited a broad glow curve consisting of a prominent peak at around 180 °C (heating rate = 5 °C/s). Fig. 3 shows the TSL glow peak for the powder. Trapping parameters were calculated using Chen's formulae [17] and they are listed in Table 1. The calculated activation energy is 0.97 eV.

Fig. 4(a) shows the ESR spectrum at room temperature after gamma irradiation (3 kGy) of $LiAl_5O_8$:Eu phosphor. The observed spectrum appears to be a superposition of at least two distinct centres. This inference is based on thermal-annealing experiments. It was possible to identify two centres and these are labelled in Fig. 4(b). The ESR line labelled as I is due to a centre characterized by a single broad line with an isotropic g-value 2.0089 and 70 G line width. In general, not many defect centres are expected to be formed in a system like $LiAl_5O_8$ and the most probable centres which can be observed are the V-centres, F-centres and F^+-centres (an electron trapped at an anion vacancy).

The large line width of centre I indicates unresolved hyperfine structure. The unresolved structure results from the interaction of the unpaired electron with nearby nuclear spins. Aluminium as well as lithium in $LiAl_5O_8$ have isotopes with nuclear spins 5/2, 3/2, 1: ^{27}Al, ^7Li and ^6Li. ^{27}Al is much more abundant (100%) than ^6Li (7.4%) and ^7Li (92.6%) and its nuclear magnetic moment is higher (3.6385) than that of ^6Li (0.8219) and ^7Li (3.256) [18]. It is likely, therefore, that the electronic spin will be interacting with aluminium ions and also possibly with lithium (^7Li) ions. It is known that the cation disorder and non-stoichiometry of aluminates provide a large number of lattice defects, which may
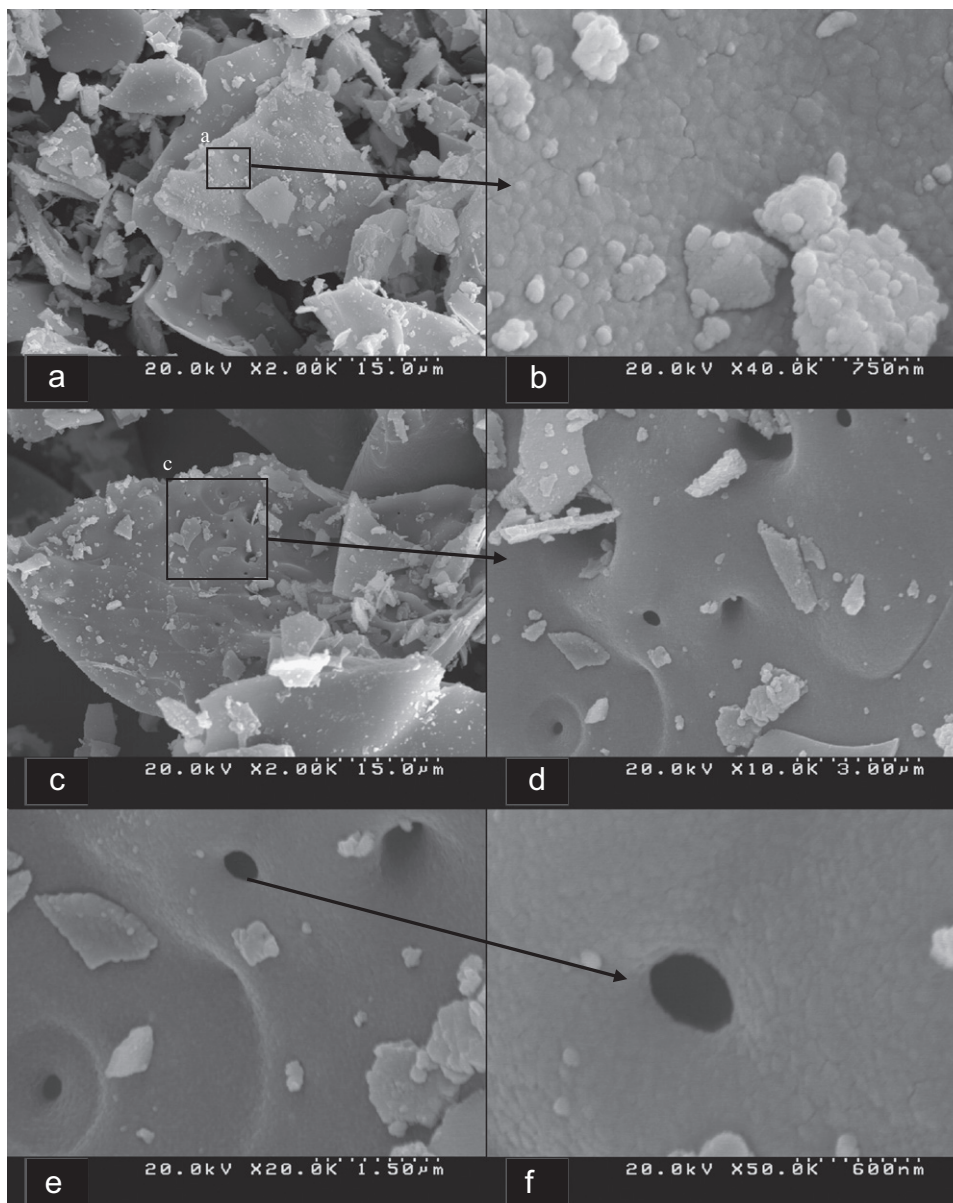
Fig. 2. SEM images of $LiAl_5O_8$:Eu.

serve as trapping centres. In such a case, oxygen vacancies should lead to F^+-centres by trapping electrons. On the other hand, hole trapping at aluminium and lithium vacancies can lead to formation of V-centres. The observed broad ESR line of centre I and the associated unresolved hyperfine structure indicates that the unpaired electron is delocalized and interacts with nearby aluminium/lithium nuclei. It has been speculated [19] that in oxides, the charges must be trapped near double (or more) charged defects in order for the charge to be delocalized, thus allowing it to interact with surrounding nuclei. Hence centre I is tentatively assigned to a V-centre—a hole trapped on an oxygen ion, forming an O^- ion, adjacent to an Al-ion/Li-ion vacancy. The observed positive g-shift of centre I is also in accordance with the expectations for a V-centre. It may be mentioned that a similar centre in neutron irradiated $MgAl_2O_4$ has also been ascribed to a V-centre [20].

The stability of centre I was measured using the pulsed thermal-annealing method. After heating the sample up to a given temperature value where it is maintained for 3 min, it is cooled rapidly down to room temperature for ESR measurements. In Fig. 4(b), centre I ESR line is seen with reduced intensity and in Fig. 4(c), the line is not visible. The thermal-annealing behaviour of centre I is shown in Fig. 5. It is observed that the centre shows two intensity decreasing stages. The first stage is in the temperature range 70–120 °C and the actual decay of the centre is taking place in the range 120–200 °C. This stage appears to relate to the TL peak at 180 °C.

The ESR line labelled as II in Fig. 4(a) is due to a centre characterized by a single ESR line with an isotropic g-value 2.0059 and 10 G linewidth. One of the most probable centre which can be trapped in the present system is the F^+-centre (an electron trapped at an anion vacancy). Hutchison [21] first observed such a centre in neutron irradiated LiF. In LiF, a single broad line (linewidth $\sim$100 G) with a g-factor 2.008 was observed. X-ray or gamma irradiation also produces such a centre in other systems like alkali halides. Such centres are characterized by (1) a small g-shift, which may be positive or negative, (2) a large linewidth and (3) saturation properties characteristic of an in homogenously broadened ESR line. Unresolved hyperfine structure causes large linewidths.
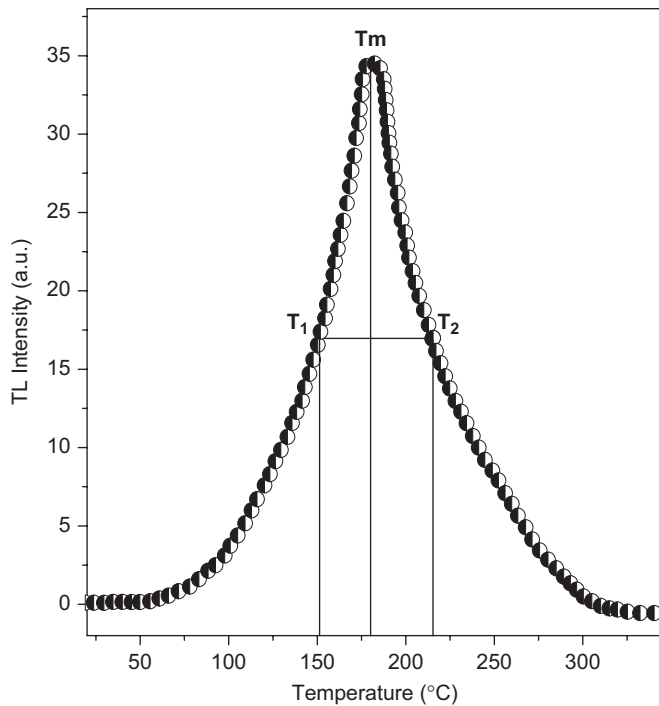
Fig. 3. Themoluminescence glow curve of $LiAl_5O_8$:Eu phosphor.

Table 1
Trapping parameters for $LiAl_5O_8$:Eu calculated from TL glow curve (dose: 1.7 kGy)

T_1 (K)	T_m (K)	T_2 (K)	μ_g	Order of kinetics	E_τ (eV)	E_δ (eV)	E_ω (eV)	E (eV)
424	453	488	0.54	2	0.98	0.96	0.97	0.97

Irradiation leads to the trapping of an electron at an anionic vacancy and such trapping is the basis for the formation of F^+-centres. Hyperfine interaction with the nearest-neighbor cations is the major contribution to the line width. Defect centre II formed in the present system is characterized by a small g-shift and the line width is reasonably large. The centre also does not exhibit any resolved hyperfine structure. On the basis of these observations and considerations of the characteristic features of the defect centres likely to be formed in a system such as $LiAl_5O_8$:Eu, centre II is tentatively assigned to a F^+-centre.

The stability of centre II was measured using the pulsed thermal-annealing technique. ESR line of centre II is seen without the interference of centre I line in Fig. 4(c). On the other hand, centre II has decayed after thermal annealing at 260 °C [Fig. 4(d)]. The thermal-annealing behaviour of centre II is shown in Fig. 6. It is observed that this centre also shows two decreasing stages. The first stage is in the temperature range 110–170 °C whilst the actual decay of the centre is in the range 170–240 °C and this decay relates to the TL peak at 180 °C. It is speculated that the thermally released electrons from the F^+-centres are recombining with holes trapped at V-centres and V-centres act as recombination centres. The recombination energy is transferred to the europium ion which act as luminescent centres emitting light.

3.4. Photoluminescence studies

Fig. 7 shows the excitation (a) and emission (b) spectra of $LiAl_5O_8$:Eu phosphor prepared by the combustion method. The
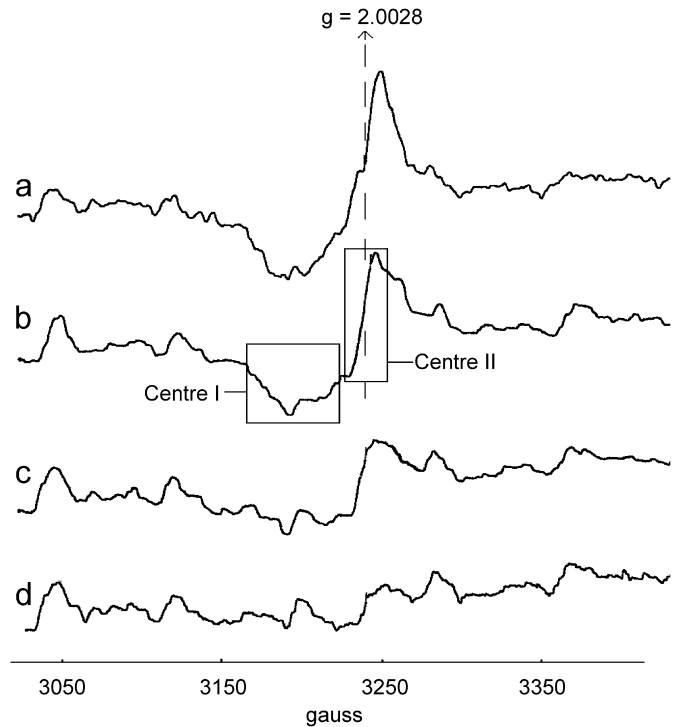

Fig. 4. Room temperature ESR spectra of irradiated $LiAl_5O_8$:Eu phosphor. (gamma dose: 3000 Gy): (a) immediately after irradiation, (b) after annealing at 120 °C—line labelled as I is due to a V-centre and (c) and (d) refer to spectra recorded after annealing at 170 and 260 °C, respectively. Centre II line is assigned to a F^+-centre.
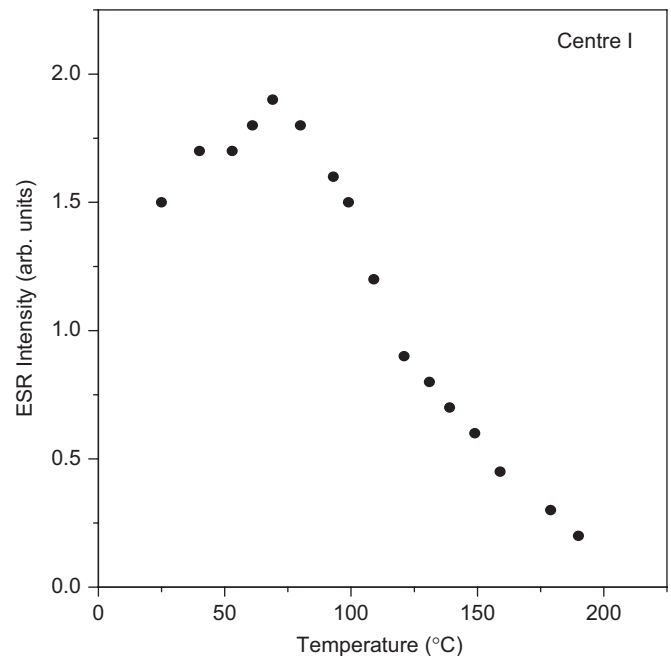

Fig. 5. Thermal-annealing behaviour of centre I in $LiAl_5O_8$:Eu phosphor.

excitation spectrum (Fig. 7(a)) consists of a broad band ranging from 200 to 500 nm with a maximum at 278 nm and some sharp lines in the longer wavelength region. The wide band at about 278 nm is attributed to the transition towards the charge transfer state (CTS) due to Eu–O interaction [22]. Apart from the charge transfer band, some sharp lines are also seen in the excitation
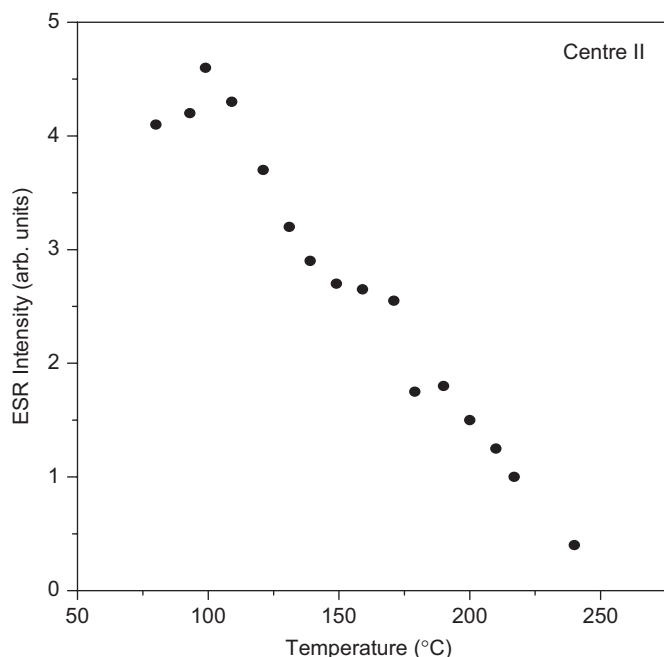
Fig. 6. Thermal-annealing behaviour of centre II in $LiAl_5O_8$:Eu phosphor.

Fig. 7. Photoluminescence spectra of the Eu-doped $LiAl_5O_8$: (a) excitation spectra of $LiAl_5O_8$:Eu and (b) emission spectra of $LiAl_5O_8$:Eu.

spectrum of Eu^{3+} which corresponds to f–f transitions. Lines at 362, 381, 395, 413, 465 nm are attributed to $^7F_0$–$^5D_4$, $^7F_0$–$^5L_7$, $^7F_0$–$^5L_6$, $^7F_0$–$^5D_3$, $^7F_0$–$^5D_2$, respectively. They originate from transitions within Eu^{3+}, $4f^6$ configuration. Usually 395 nm band is known to provide the most intense excitation peak. In this case two prominent peaks are observed at 395 and 465 nm without any big difference in the intensities.

Fig. 7(b) displays the emission spectra of the europium-doped $LiAl_5O_8$ phosphor that are measured as the function of different excitation wavelengths observed in the excitation profile of Fig. 7(a). The emission spectra contain the characteristic $^5D_0$–^7F_J ($J = 0, 1, 2, 3, 4$) emission of Eu^{3+}, i.e. emission at 576 nm ($^5D_0$–$^7F_0$), 588 nm ($^5D_0$–$^7F_1$), 613 nm ($^5D_0$–$^7F_2$), 651 nm ($^5D_0$–$^7F_3$) and 700 nm ($^5D_0$–$^7F_4$). Among them, 613 nm ($^5D_0$–$^7F_2$) is the most prominent emission. In particular, the red emission ($^5D_0$–$^7F_2$) is considered as a hypersensitive transition which obeys the selection rule of $\Delta J = 2$ and hence, it demonstrates a bright emission. The peak from $^5D_0$ to $^7F_2$ (electric–dipole transition) is stronger than that from $^5D_0$ to $^7F_1$ (magnetic–dipole transition), indicating the absence of inversion symmetry of the sites occupied by the Eu^{3+} ions. So the sites in the $LiAl_5O_8$ are occupied by Eu^{3+} ions that have no inversion symmetry. In addition, we have also found that there is the lack of splitting in other weaker emission transitions. However, $LiAl_5O_8$ is known to have spinel structure and the most favourable distribution would correspond to $(Li_xAl_{2-x})^t$ $(Li_{1-x} Al_{3+x})^oO$ (t = tetrahedral and O = octahedral; where $x = 0.13$–0.33) [23]. It is known that in $LiAl_5O_8$, the lattice contains LiO_4, LiO_6, AlO_4 or AlO_6 groups. There has been debate on the cationic distribution in $LiAl_5O_8$, particularly about the site occupancy of Li; it is singularly octahedral or occupies both octahedral and tetrahedral sites. Kordes [24] proposed the spinel structure as well as primitive cubic for $LiAl_5O_8$ wherein Li^+ and part of Al^{3+} together occupied the position of both octahedral as well as tetrahedral sites. Therefore, in the present study, it is very difficult to say whether Eu substitutes Li or Al or both ions. In order to resolve the issue of Eu substitution there is need of more studies. The orange red/red emission of the prepared $LiAl_5O_8$:Eu phosphor indicates that its probable utility for photoluminescence liquid crystal display (PLLCD) application.
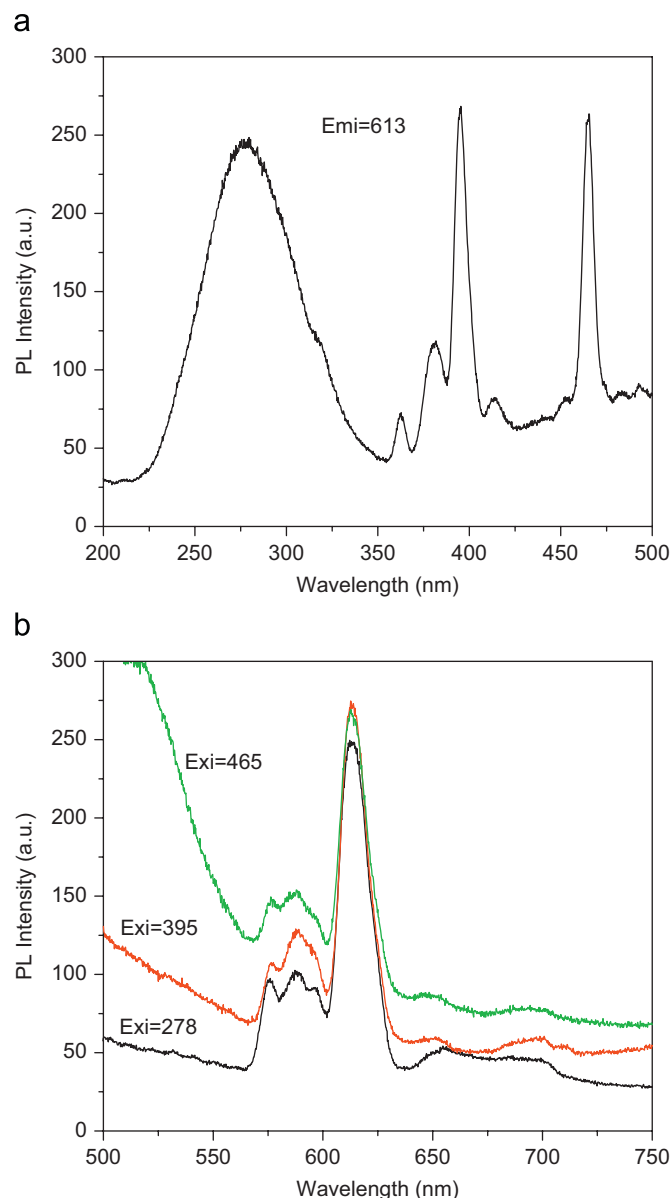
4. Conclusions

Based on the results presented above, the following conclusions may be highlighted:

1. In this work, we have prepared red emitting $LiAl_5O_8$:Eu^{3+} phosphor in one step by the combustion synthesis. The synthesis is rapid and carried out at the furnace temperature as low as 500 °C. Powder X-ray diffraction (XRD) indicated the presence of mono-$LiAl_5O_8$ phase.
2. TL glow peak was observed in gamma-irradiated europium ion-doped sample at around 180 °C.
3. Two defect centres are identified in irradiated $LiAl_5O_8$:Eu phosphor and these centres are tentatively assigned to V-centre and F^+-centre.
4. V-centre and also F^+-centre appear to correlate with the 180 °C TL peak.
5. The photoluminescence spectra of $LiAl_5O_8$:Eu^{3+} showed prominent red emission located at about 613 nm and is ascribed to

$^5D_0$–$^7F_2$ transition of Eu^{3+} ions. High-resolution SEM micrographs show the presence of several micro and nanoparticles within the grains.

References

[1] L. Zuwu, L. Xi, L. Jun, Nat. Sci. J. Xiangtan. Univ. 18 (1996) 49.

[2] T.R.N. Kutty, M. Nayak, J. Alloys Compd. 269 (1998) 75.

[3] Xiulan Duan, Duorong Yuan, J. Non-Cryst. Solids 351 (2005) 2348.

[4] Dongying Pan, Duorong Yuan, Haiqing Sun, Xiulan Duan, Caina Luan, Shiyi Guo, Zhanfa Li, Lihua Wang, Mater. Chem. Phys. 96 (2006) 317.

[5] U. Rambabu, T. Balaji, S. Buddhudu, Mater. Res. Bull. 30 (1995) 891.

[6] T. Justel, J.C. Krupa, D.U. Wiechert, J. Lumin. 93 (2001) 179.

[7] C. Louis, R. Bazzi, A. Marco, W. Flores, K. Zheng, O. Lebbou, B. Tillement, C. Mercier, P. Dujardin, J. Perriat, Solid State Chem. 173 (2003) 335.

[8] P.M. Guo, F. Zhao, G.B. Li, F.H. Liao, S.J. Tian, X.P. Jing, J. Lumin. 105 (2003) 61.

[9] S.J. Dhoble, S.V. Moharil, T.K. Gundu Rao, J. Lumin. 93 (2001) 43.

[10] S. Murali, V. Natarajan, R. Venkataramani, Pushparaja, M.D. Sastry, Appl. Radiat. Isot. 55 (2001) 253.

[11] S. Murali, V. Natarajan, T.K. Seshagiri, R.M. Kadam, R. Venkataramani, M.D. Sastry, Radiat. Meas. 37 (2003) 259.

[12] Vijay Singh, T.K. Gundu Rao, Jun-Jie Zhu, J. Solid State Chem. 179 (2006) 2574.

[13] Vijay Singh, T.K. Gundu Rao, Jun-Jie Zhu, Manoj Tiwari, Mater. Sci. Eng. B 131 (2006) 195.

[14] Vijay Singh, T.K. Gundu Rao, Jun-Jie Zhu, J. Lumin 126 (2007) 1.

[15] S.R. Jain, K.C. Adiga, V.R. Pai Vernekar, Combust. Flame 40 (1981) 71.

[16] Vijay Singh, R.P.S. Chakradhar, J.L. Rao, Dong-Kuk Kim, J. Lumin., communicated.

[17] R. Chen, J. Electrochem. Soc. 116 (1969) 1254.

[18] R.C. Weast (Ed.), Handbook of Chemistry and Physics, CRC, Cleveland, 1971.

[19] N.Y. Konstantinov, L.V. Karaseva, V.V. Gromov, Dokl. Acad. Nauk. SSR 228 (1980) 631.

[20] V.T. Gritsyna, V.A. Kobyakov, Zh. Tekh. Fiz 55 (1985) 354 (Sov. Phys. Tech. Phys. 30(1985)206).

[21] C.A. Hutchison, Phys. Rev. 75 (1949) 1769.

[22] G. Liu, G. Hong, D. Sun, J. Colloid. Interface Sci. 278 (2004) 133.

[23] N.T. Melamed, F.deS. Barros, P.J. Viccaro, J.O. Artman, Phy. Rev. B 5 (1972) 3377.

[24] E. Kordes, Z. F. Kristallogr. 91 (1935) 193.